

# An Autonomous Piezoelectric Shunt Damping System

Andrew J. Fleming, Sam Behrens, and S. O. Reza Moheimani

School of Electrical Engineering and Computer Science, The University of Newcastle,  
Callaghan 2308, Australia.

## ABSTRACT

Passive shunt damping involves the connection of an electrical shunt network to a structurally attached piezoelectric transducer. In recent years, a large body of research has focused on the design and implementation of shunt circuits capable of significantly reducing structural vibration. This paper introduces an efficient, light weight, and small-in-size technique for implementing piezoelectric shunt damping circuits. A MOSFET half bridge is used together with a signal processor to synthesize the terminal impedance of a piezoelectric shunt damping circuit. Along with experimental results demonstrating the effectiveness of switched-mode shunt implementation, we discuss the design of a device aimed at bridging the gap between research in this area and practical application.

**Keywords:** Piezoelectric, Switched-Mode, Impedance, Synthesis, Shunt, Damping, Vibration, Suppression, Embedded

## 1. INTRODUCTION

Passive shunt damping involves the connection of an electrical shunt network to a structurally attached piezoelectric transducer. By means of the piezoelectric electro-mechanical coupling, the passive network is capable of damping structural vibration.

In recent years, the design and implementation of suitable shunt circuits has been an ongoing topic of research. Descending from the early work by Hagood and von Flotow<sup>1</sup>, single-mode resonant shunting techniques have been extended to allow for multiple structural modes<sup>2,3</sup>, variable resonance frequencies<sup>4</sup>, and lower circuit inductance values<sup>5</sup>. Due to the impractically large inductance values that are typically required, such resonant shunt circuits have been implemented using discrete resistors, virtual inductors, and Riodan Gytrators<sup>6</sup>. The synthetic impedance<sup>7,8</sup>, a new approach to electrical network synthesis, has eliminated many of the problems associated with previous techniques such as circuit complexity, internal voltage limitations, and tuning difficulties.

In parallel to resonant shunting techniques, work has also progressed on the so called *switched shunt* or *switched stiffness* techniques<sup>9</sup>. Three major subclasses exist where the piezoelectric element is switched in and out of a shunt circuit comprising either: another capacitor<sup>10</sup>, a resistor<sup>11</sup>, or an inductor<sup>12</sup>. The required inductance is typically one tenth of that required to implement a simple  $L - R$  resonant shunt circuit designed to damp the same mode. To their detriment, such techniques are applicable only to single degree of freedom structures or structures with sinusoidal excitation. As with virtual circuit implementation, an external power source is required for the gate drive and timing electronics.

This paper first introduces a new method for implementing an arbitrary terminal admittance. The switched mode synthetic admittance requires no high voltage linear components, is small in size, and is ideal for implementing industrial scale shunt damping systems with large excitation. The device is capable of recycling reactive power and when compared to opamp based techniques, requires only a miniscule operating current.

This paper also discusses the design of a miniature embedded high voltage device aimed at practical active noise and vibration control problems. The prototype, containing an analog acquisition system, DSP, and high voltage amplifier is to be small in size, use little power, and be mechanically and electrically robust.

---

(Send correspondence to [andrew@ee.newcastle.edu.au](mailto:andrew@ee.newcastle.edu.au))

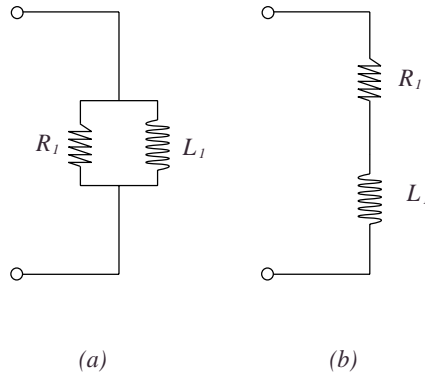


**Figure 1.** Parallel (a) and series (b) single mode shunt damping circuits.

### 1.1. Piezoelectric Shunt Damping

Single mode damping was introduced to decrease the magnitude of one structural mode<sup>13</sup>. Two examples of single mode damping are shown in Figure 1, parallel and series shunt damping. An  $R-L$  shunt circuit introduces an electrical resonance, this can be tuned to one structural mode in a manner analogous to that of a mechanical vibration absorber. Single mode damping can be applied to reduce several structural modes with the use of as many piezoelectric patches and damping circuits.

Problems may result if the piezoelectric patches are bonded to, or imbedded in the structure. First, the structure may not have sufficient room to accommodate all of the patches. Second, the structure may be altered or weakened when the piezoelectric patches are applied. In addition, a large number of patches can increase the structural weight, making it unsuitable for applications such as aerospace.

To alleviate the problems associated with single mode damping, multi-mode shunt damping has been introduced, i.e. the use of one piezoelectric patch to damp multiple structural modes. Several techniques have emerged:

- Current blocking techniques, as presented in<sup>2</sup>, are based on placing a number of single mode  $R-L$  branches in parallel, one for each mode to be controlled. Each branch also requires the addition of a parallel  $L-C$  current blocking network to isolate the effect of each branch to a single mode.
- Current flowing techniques, as presented in<sup>3</sup>, are similar to current blocking techniques, a number of single mode branches are connected in parallel. Current flowing networks are used in place of the current blocking networks to isolate adjacent branches. Current flowing shunt damping circuits are lower in order than current blocking circuits and hence, prove useful for damping a large number of modes
- By considering the underlying feedback structure associated with piezoelectric shunt damping<sup>14</sup>, a suitable controller is first designed, then used to identify the corresponding shunt admittance.

Typical shunt circuits require large inductance values of up to thousands of Henries. Virtual grounded and floating inductors (Riordan gyrators<sup>6</sup>) are required to implement the inductor elements. Such virtual implementations are large in size, difficult to tune, and are sensitive to component age, temperature, and non-ideal characteristics.

Piezoelectric patches are capable of generating hundreds of volts for moderate structural excitations. This requires the entire circuit be constructed from high voltage components. Further voltage limitations arise due to the internal gains of the virtual inductors.

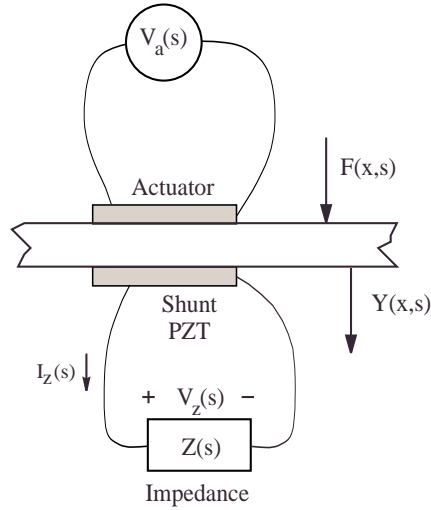


**Figure 2.** Structural inputs / outputs.

## 1.2. Modelling the Compound System

For generality, we enter the modelling process with knowledge *a priori* of the system dynamics. As an example we will consider a simply supported beam with two bonded piezoelectric patches, one to be used as a source of disturbance, and the other for shunt damping. The transfer function  $G_{vv}(s)$  measured from the applied actuator to sensor voltage can be derived analytically from the Euler-Bernoulli beam equation<sup>15</sup>, or alternatively, obtained experimentally through system identification<sup>16,17</sup>. Using similar methods, we may obtain the transfer function from an applied actuator voltage to the resulting displacement at a point  $G_{yv}(x, s)$ . Consider Figure 2 where a piezoelectric patch is shunted by an impedance  $Z(s)$ . In reference<sup>14</sup>, the damped system transfer functions  $\tilde{G}_{vv}(s)$ , and  $\tilde{G}_{yv}(x, s)$  are shown to be,

$$\tilde{G}_{vv}(s) \triangleq \frac{V_s(s)}{V_a(s)} = \frac{G_{vv}(s)}{1 + G_{vv}(s)K(s)}. \quad (1)$$

$$\tilde{G}_{yv}(x, s) \triangleq \frac{Y(x, s)}{V_a(s)} = \frac{G_{yv}(x, s)}{1 + G_{vv}(s)K(s)}. \quad (2)$$

where  $K(s) = \frac{Z(s)}{Z(s) + \frac{1}{C_p s}}$ . Note that  $V_p(s)$  is dynamically equivalent to  $V_s(s)$  (i.e. the open circuit voltage). Using a similar procedure and the principle of superposition, the effect of a generally distributed disturbance force can be included<sup>14</sup>.

## 2. THE SWITCHED MODE SYNTHETIC ADMITTANCE

The switched mode synthetic admittance will be introduced as an alternative to the synthetic admittance<sup>7,8</sup>.

### 2.1. Device Operation

A simplified circuit diagram of the switched mode admittance is shown in Figure 3. The basic idea is the same as that discussed previously, the device attempts to maintain some arbitrary relationship between voltage and current at its terminals, i.e. between  $i_T$  and  $v_T$ .

We begin with some preliminary circuit analysis. In the Laplace domain,

$$I_T(s) = \frac{V_T(s) - V_{pwm}(s)}{Z_c(s)}. \quad (3)$$

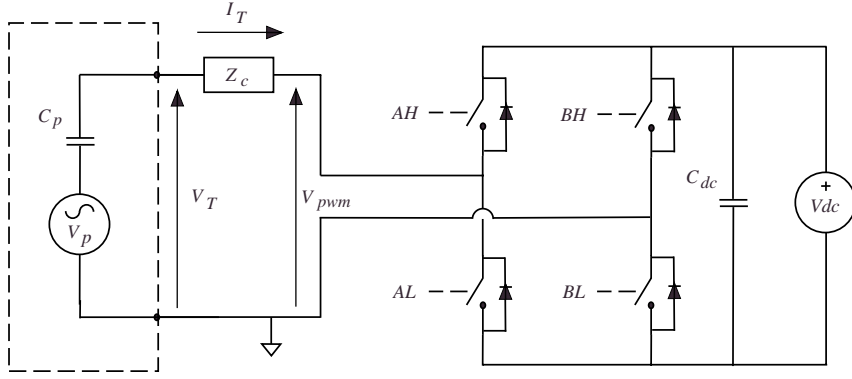


**Figure 3.** The switched mode synthetic admittance.

We desire the terminal voltages and currents to be related by some arbitrary function, in this case a terminal impedance  $Z_T$ .

$$I_T(s) = \frac{1}{Z_T(s)} V_T(s) \quad (4)$$

Combining (3) and (4) yields the relationship required to maintain (4) at the terminals,

$$V_{pwm}(s) = V_T(s) \left( 1 - \frac{Z_c(s)}{Z_T(s)} \right). \quad (5)$$

The reader may recognize the similarity between the circuit on the right hand side of Figure 3 and a controlled single phase switch mode rectifier, or a four quadrant switched mode amplifier. Indeed, the only difference between such devices is the selection of the control impedance and the bridge control algorithm. Although we cannot synthesize  $v_{pwm}(t)$  exactly, we can do so in the average sense. The relationship between the reference signal and the control duty cycle is  $D = \frac{1}{2} \left( \frac{v_{ref}}{V_{dc}} + 1 \right)$ .

The principle of operation is explained fairly simply. The desired terminal current (a function of the terminal voltage) is synthesized by controlling the average voltage across the impedance  $Z_c$ .

### 2.1.1. Boost Configuration

In this section we consider a specific choice for the control impedance  $Z_c$ , a series connection of an inductor and resistor. In this configuration, the structure of the circuit resembles that of a single phase boost rectifier. The primary motivation is to allow the flow of real and reactive power back to the source.

Assuming that the inductance is large enough to maintain an approximately constant current over the switching interval, when the applied potential  $v_{pwm}$  opposes the current  $i_T$ , the inductor overcomes the source potential and forces the current to flow through the anti-parallel diodes back to the source.

This configuration also has the advantage of greatly reducing the high frequency content applied to the piezoelectric transducer. The inherent capacitance of the PZT together with the control impedance creates a second order resonant low pass power filter.

$$V_T(s) = \frac{\frac{1}{L_c C_p}}{s^2 + \frac{R_c}{L_c} s + \frac{1}{L_c C_p}} V_{pwm}(s) \quad (6)$$

For reasonable values of  $R_c$ ,  $L_c$ , and  $C_p$  ( $300 \Omega$ ,  $0.1 H$ ,  $400 \mu F$ ), the filter has a cutoff frequency of around  $800 Hz$ . If we consider a system with a switching frequency of  $8 kHz$ , such a filter would attenuate the fundamental switching component by  $40 dB$ . Taking into account the additional low pass dynamics of the plant, the actual realized disturbance due to switching is negligible.

## 2.2. Efficiency

If we consider a sinusoidal voltage source  $V_s$  connected to an impedance  $Z_T$ , the real dissipated power is

$$P_T = \frac{1}{2} |V_s|^2 \operatorname{Re} \left\{ \frac{1}{Z_T} \right\} = \frac{1}{2} \left| \frac{V_s}{Z_T} \right|^2 \operatorname{Re} \{Z_T\} \quad (7)$$

We define the efficiency of the switch mode synthetic admittance as the ratio of power absorbed by  $V_{dc}$ , to the power that would normally be dissipated if the impedance  $Z_T$  was implemented using ideal physical components,  $\eta(Z_c, Z_T, \omega) = 100\% \times \frac{P_{V_{dc}}}{P_T}$ . Virtual or linear synthetic implementations will always result in a negative efficiency, i.e., they absorb no real power. In fact, the situation is worse, such implementations must actually supply power to synthesize the flow of apparent power. For our application, i.e., synthesizing inductors to form a highly resonant circuit, the realized efficiency is extremely poor (large and negative).

The quantity  $P_{V_{dc}}$  is computed easily for the boost configuration by performing a power balance. Obviously, the real power as seen from the terminals will be equal to  $P_T$ . The only remaining contribution to the net real power flow is the control impedance,

$$P_c = \frac{1}{2} \left| \frac{V_s}{Z_T} \right|^2 \operatorname{Re} \{Z_c\} \quad (8)$$

$$\eta(Z_c, Z_T, j\omega) = 100\% \times \frac{P_T - P_c}{P_T} \quad (9)$$

$$= 100\% \times \left[ 1 - \frac{\operatorname{Re} \{Z_c\}}{\operatorname{Re} \{Z_T\}} \right]. \quad (10)$$

The best efficiency (100%) is achieved if the control impedance contains no real component. If the control impedance has a larger real component than the terminal impedance, the efficiency is negative, i.e., the source  $V_{dc}$  must supply real power to the system.

## 2.3. Practical Advantages and Considerations

The switched mode synthetic admittance has a number of advantages over its linear counterpart. Some difficulties also arise that are not present in the linear case.

- **Cost.** Discrete power switches can be obtained for a fraction of the cost of HV linear components.
- **Size / Density.** The switching circuit shown in Figure 3 does not dissipate any real or reactive power flowing between the source and the controlling impedance. There is also no requirement for quiescent or bias current. Coupled with the small physical size of power switches, a low heat dissipation allows the circuit to be manufactured in an extremely small enclosure. Another significant factor is the size of the power supply. In the linear case, a large supply is required to power the components and to supply reactive power to the structure. As we have seen, in the switching case, not only is the power supply small, but if the synthesized terminal impedance has a larger real component than the controlling impedance, no power supply is required at all.

- **Control Conditioning.** The switched mode synthetic admittance manipulates the terminal current by controlling the average voltage across a control impedance  $Z_c$ . In practice, the problem must be conditioned so that the expected current range results in realizable voltage differences across the control impedance. We can derive the voltage conditioning ratio,  $\frac{V_{pwm}(s)}{V_T(s)} = 1 - \frac{Z_c(s)}{Z_T(s)}$ . At a specific frequency, the problem is easily conditioned by ensuring  $|Z_c(s)| \gg |Z_T(s)|$ , i.e., by choosing a control impedance much greater in magnitude than  $Z_T(s)$ . Another simple technique is to design  $Z_c(s)$  having an opposite or significantly different phase angle with respect to  $Z_T(s)$ . In the boost configuration, we are limited in choice to an inductor and resistor.

The impedance of passive shunt damping circuits is typically comprised of inductive resistive branches. In the active frequency range, the reactance of each branch is heavily dominated by the inductor, this is expected as resonant circuits operate at very low power factors (implying small real impedance).

We must consider a number of factors: For efficiency we wish to keep the control resistance  $R_c$  small. If  $R_c$  is small, the only way to increase the control impedance, is to increase the size of the inductance  $L_c$ . As both the control and terminal impedance have a similar impedance angle (approximately  $+\pi$ ), we cannot improve the control conditioning by relying on a phase difference. Thus, to obtain a well conditioned voltage drop across the control impedance  $Z_T$ , the control inductance must be a reasonable fraction of the terminal inductance. e.g.,  $L_c = \frac{L_T}{10}$ . Multi-mode shunt circuits include at least one inductance per branch, in this case, we must consider the lowest frequency branch, (the branch with the greatest inductance). All higher frequency branches will have an improved condition ratio.

- **Common Mode Instrumentation Performance.** The operation of the circuit requires the return terminals of the PZT and  $V_{dc}$  to be electrically isolated. Preferably, the acquisition of  $v_T$  should be performed using a circuit completely isolated from both references. As this is impossible in practice, the instrumentation amplifier must have a high common mode rejection ratio to attenuate components resulting from the varying potential between the two references.

### 3. POWER HARVESTING

The switched mode synthetic admittance is capable of absorbing energy from an electrical source. When the efficiency (10) is positive, and the device is being used to implement some network containing a finite resistance, the net real power flow into the DC source is also positive.

According to<sup>4</sup>, the damped system transfer function from an applied actuator voltage to the measured output  $V_z$ , is

$$G_{v_z v} = \frac{V_z(s)}{V_a(s)} = \frac{K(s)G_{vv}(s)}{1 + K(s)G_{vv}(s)} \quad (11)$$

where  $K(s)$  is defined in Section 1.2. Given the damped terminal voltage (11), and the operating efficiency (10), we can quantify the harvested real power. At a specific frequency, the real power dissipated by the terminal impedance is,

$$P_T(j\omega) = \frac{1}{2} |V_z(j\omega)|^2 \mathbf{Re} \left\{ \frac{1}{Z_T(j\omega)} \right\} \quad (12)$$

thus,

$$\begin{aligned} P_{V_{dc}}(j\omega) &= \eta \frac{1}{2} \left| \frac{V_z(j\omega)}{Z_T(j\omega)} \right|^2 \mathbf{Re} \{ Z_T(j\omega) \} \\ &= \frac{1}{2} \left| \frac{V_z(j\omega)}{Z_T(j\omega)} \right|^2 [\mathbf{Re} \{ Z_T(j\omega) - Z_c(j\omega) \}] \end{aligned} \quad (13)$$

where  $V_z(s) = G_{v_z v}(s)V_a(s)$ , and  $\eta$  denotes  $\eta(Z_c, Z_T, j\omega)$ .

Length, $L$	0.6 $m$
Width, $w_b$	0.05 $m$
Thickness, $h_b$	0.003 $m$
Youngs Modulus, $E_b$	$65 \times 10^9 \text{ N/m}^2$
Density, $\rho$	2650 $kg/m^2$

**Table 1.** Experimental Beam Parameters

Length	0.070 $m$
Charge Constant, $d_{31}$	$-210 \times 10^{-12} \text{ m/V}$
Voltage Constant, $g_{31}$	$-11.5 \times 10^{-3} \text{ Vm/N}$
Coupling Coefficient, $k_{31}$	0.340
Capacitance, $C_p$	0.105 $\mu F$
Width, $w_s \ w_a$	0.025 $m$
Thickness, $h_s \ h_a$	$0.25 \times 10^{-3} \text{ m}$
Youngs Modulus, $E_s \ E_a$	$63 \times 10^9 \text{ N/m}^2$

**Table 2.** Piezoelectric Transducer Properties

## 4. EXPERIMENTAL RESULTS

The switched mode synthetic admittance will now be employed to implement a two mode current blocking piezoelectric shunt damping circuit designed to damp the second and third modes of an experimental simply supported beam. In theory, the circuit is capable of harvesting power from the structure. To date, practical difficulties have avoided such operation.

The problems with power harvesting are due mainly to the highly reactive nature of piezoelectric shunt damping circuits. In the frequency range of interest, the impedance of a typical shunt circuit results in a net power flow that is 90-99 % reactive. Thus, to harvest power, the device must efficiently recycle reactive power and absorb only the minute amount of real power normally dissipated by the resistance. In practice, losses due to switching, imperfect boost inductors, and other parasitic effects prevent such ideal operation.

### 4.1. Experimental Setup

The experimental beam is a uniform aluminum bar with rectangular cross section and experimentally pinned boundary conditions at both ends. A pair of piezoelectric ceramic patches (PIC151) are attached symmetrically to either side of the beam surface. One patch is used as an actuator and the other as a shunting layer. Physical parameters of the experimental beam and piezoelectric transducers are summarized in Tables 1 and 2. Note that the location of the piezoelectric patch offers little control authority over the first mode. In this work, the structures second and third modes are targeted for reduction.

The displacement and voltage frequency responses are measured using a Polytec scanning laser vibrometer (PSV-300) and a HP spectrum analyzer (35670A).

### 4.2. Damping Performance

In reference<sup>8</sup>, a piezoelectric shunt damping circuit is designed to minimize the  $\mathcal{H}_2$  norm of the compound beam described in Section 4.1. The switched mode admittance, with a control impedance of  $67 \text{ mH} + 33 \text{ k}\Omega$ , is connected to the piezoelectric transducer and used to implement the shunt circuit.

The experimental open and closed loop transfer functions from an applied actuator voltage to the displacement at a point  $G_{yv}(x = 0.17 \text{ m}, s)$  are shown in Figure 4. The amplitudes of the second and third modes are reduced by 21.6 and 21.3  $dB$  respectively.

To analyze the linearity of the switched mode implementation, a sine wave was applied at the second mode resonance frequency, the power spectral density of the resulting voltage applied to the piezoelectric transducer is shown in Figure 5. The harmonic content and switching noise applied to the piezoelectric transducer is negligible ( $j$  60  $dB$ ).

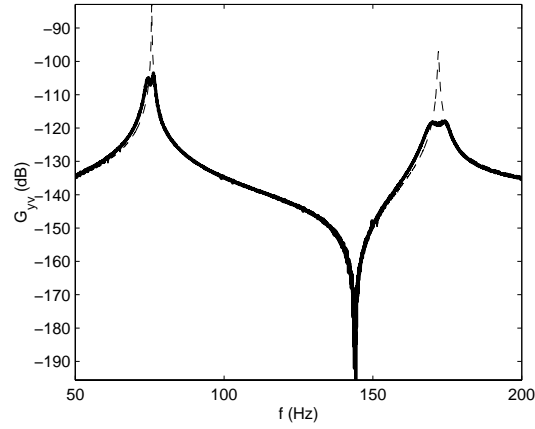


**Figure 4.** Experimental open loop (- -) and damped system transfer (—) functions.

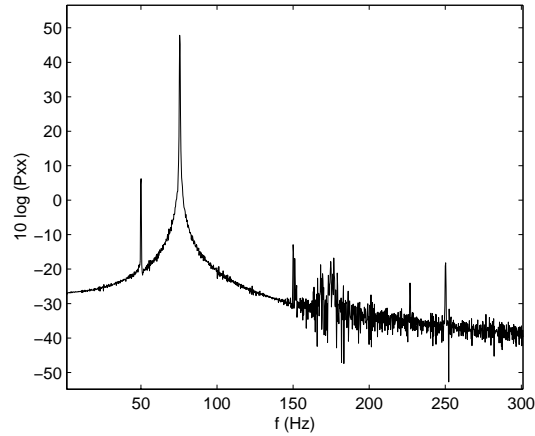


**Figure 5.** Power spectral density of the terminal voltage  $V_z$  applied to the piezoelectric transducer.

## 5. EMBEDDED IMPLEMENTATION

The necessary functionality required to implement a HV piezoelectric shunt damping system is shown in Figure 6.

An embedded DSP controller containing a processor, analog to digital converter (ADC), and pulse width modulator (PWM), implements the required signal processing and gate signal generation. Alternatively, this function could also be realized with an analog signal filter and discrete PWM modulator. Apart from the low ADC resolution, the TI320LF2403A 16 bit fixed-point embedded control DSP is an ideal choice. The device is capable of low-power 40 MIPS processing, contains an ample amount of ROM and RAM, and amongst additional peripherals, also contains a timer module dedicated to PWM generation. The required board space is  $12 \times 12 \text{ mm}$ .

The switch-mode amplifier, supplied by a miniature HV DC-DC converter, and containing a MOSFET H-Bridge, gate drive circuitry, and opto-isolator, is connected through the control impedance  $Z_c$  to the piezoelectric transducer. Given the small amount of real power required, 500 V operation can be achieved with a  $12.5 \times 12.5 \text{ mm}$  1.25 W DC-DC converter.

The aim is to fit the entire system including connectors and a programming port onto a board  $70 \times 25 \text{ mm}$ .

## 6. CONCLUSIONS

Piezoelectric shunt damping circuits require impractically large inductors. A large improvement over virtual circuit implementations was achieved with the introduction of the synthetic admittance. The switched mode

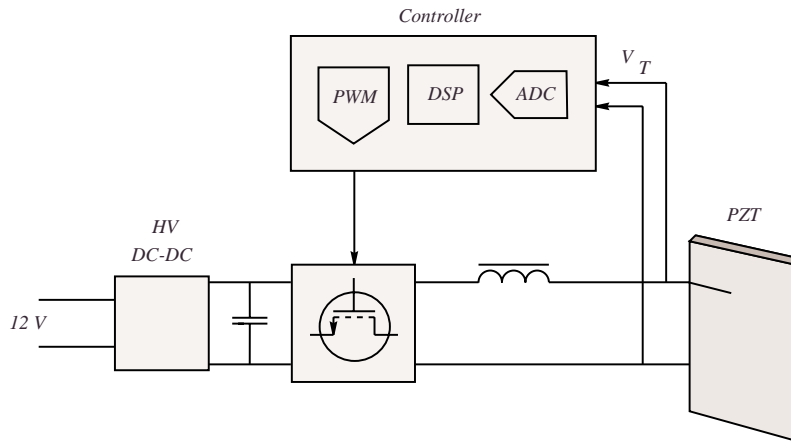


**Figure 6.** Functional diagram of an embedded switched mode impedance.

admittance has been presented as a low cost, high voltage, and extremely efficient alternative to its linear complement.

Because the load is almost purely capacitive, the combination of the load and the control impedance can be designed as a low pass power filter. This allows highly linear synthesis of the voltage  $V_z$  applied to the piezoelectric transducer with negligible harmonic or switching components.

By implementing a current-flowing shunt circuit, two modes of a simply supported beam were successfully reduced in amplitude by 21.6 and 21.3 *dB*.

Although, ideally, the device is capable of harvesting power when implementing a circuit with non-zero resistance, the difficulties involved when attempting to synthesize a highly reactive impedance precludes such operation. Even without the ability to power harvest, the benefits of the switched mode synthetic impedance in cost, size, weight, and power efficiency make it an extremely attractive alternative for practical implementation of piezoelectric shunt damping circuits.

Work is continuing on the design and construction of an embedded switched mode piezoelectric shunt damping system.

**Acknowledgement.** This research was supported in part by the Australian Research Council under Discovery grant DP0209396, and in part by the University of Newcastle RMC project grant.

## REFERENCES

1. N. W. Hagood and A. Von Flotow, "Damping of structural vibrations with piezoelectric materials and passive electrical networks," *Journal of Sound and Vibration* **146**(2), pp. 243–268, 1991.
2. S. Y. Wu, "Method for multiple mode shunt damping of structural vibration using a single PZT transducer," in *Proc. SPIE Smart Structures and Materials, Smart Structures and Intelligent Systems, SPIE Vol.3327*, pp. 159–168, (Huntington Beach, CA), March 1998.
3. S. Behrens and S. O. R. Moheimani, "Current flowing multiple mode piezoelectric shunt dampener," in *Proc. SPIE Smart Materials and Structures, Paper No. 4697-24*, pp. 217–226, (San Diego, CA), March 2002.
4. A. J. Fleming and S. O. R. Moheimani, "Adaptive piezoelectric shunt damping," *IOP Smart Materials and Structures* **12**, pp. 36–48, January 2003.
5. A. J. Fleming and S. O. R. Moheimani, "Reducing the inductance requirements of piezoelectric shunt damping circuits," *IOP Smart Materials and Structures* **12**, pp. 57–64, January 2003.

6. R. H. S. Riodan, "Simulated inductors using differential amplifiers," *Electronics Letters* **3**(2), pp. 50–51, 1967.
7. A. J. Fleming, S. Behrens, and S. O. R. Moheimani, "Synthetic impedance for implementation of piezoelectric shunt-damping circuits," *Electronics Letters* **36**, pp. 1525–1526, August 2000.
8. A. J. Fleming, S. Behrens, and S. O. R. Moheimani, "Optimization and implementation of multi-mode piezoelectric shunt damping systems," *IEEE/ASME Transactions on Mechatronics* **7**, pp. 87–94, March 2002.
9. L. R. Corr and W. W. Clark, "Comparison of low-frequency piezoelectric switching shunt techniques for structural damping.," *IOP Smart Materials and Structures* **11**, pp. 370–376, 2002.
10. C. L. Davis and G. A. Lesieutre, "An actively tuned solid-state vibration absorber using capacitive shunting of piezoelectric stiffness," *Journal of Sound and Vibration* **232**(3), pp. 601–617, 2000.
11. W. W. Clark, "Vibration control with state-switched piezoelectric materials," *Journal of intelligent material systems and structures*. **11**, pp. 263–271, April 2000.
12. C. Richard, D. Guyomar, D. Audigier, and H. Bassaler, "Enhanced semi-passive damping using continuous switching of a piezoelectric devices on an inductor.," in *Proc. SPIE Smart Structures and Materials, Damping and Isolation, SPIE Vol.3989*, pp. 288–299, (Newport Beach, CA), March 2000.
13. N. W. Hagood and E. F. Crawley, "Experimental investigation of passive enhancement of damping for space structures," *Journal of Guidance, Control and Dynamics* **14**(6), pp. 1100–1109, 1991.
14. S. O. R. Moheimani, A. J. Fleming, and S. Behrens, "On the feedback structure of wideband piezoelectric shunt damping systems," *IOP Smart Materials and Structures* **12**, pp. 49–56, January 2003.
15. C. R. Fuller, S. J. Elliott, and P. A. Nelson, *Active Control of Vibration*, Academic Press, 1996.
16. L. Ljung, *System Identification: Theory for the User*, Prentice Hall, 1999.
17. T. Mckelvy, H. Akcay, and L. Ljung, "Subspace based multivariable system identification from frequency response data," *IEEE Transactions on Automatic Control* **41**, pp. 960–978, July 1996.